Thermoreversible gelation of hydroxypropylmethylcellulose in simulated body fluids

S.Q. Liu, Sunil C. Joshi *, Y.C. Lam, K.C. Tam

School of Mechanical and Aerospace Engineering, Nanyang Technological University, Singapore 639798, Singapore

Abstract

The thermoreversible gelation of hydroxypropylmethylcellulose (HPMC) in simulated intestinal/gastric fluids (SIF/SGF) was monitored by microcalorimetry (micro-DSC), turbidity and rheometry. Both SGF and SIF facilitated sol–gel transition in HPMC without changing the patterns of gelation behavior. The sol–gel transition was found to be an entropy driven and temperature dependent process. Solution isotopic effects using Deuteraed water (D_2O) yielded a linear decrease in the temperature of endothermic maximum (T_{max}) with the increase in the molar ratio of D_2O, indicating that polymer–polymer direct hydrogen bonding (interchain hydrogen bonding) was involved in the gelation process in addition to hydrophobic association. It was found that the T_{max} shifted roughly linear to lower temperature with the increase of SGF/SIF content. This effect can be interpreted by the salting-out effect. Three distinct regions of the enthalpy and entropy changes (ΔH and ΔS) depending on buffer content were observed. However, ΔH and ΔS were linear with HPMC weight concentration. The aqueous solutions of HPMC showed a low critical solution temperature (LCST) and form an elastic gel with increasing temperature. Rheological measurements indicated that the sol–gel transition proceeded in two stages. The gel elasticity was affected by the polymer concentration and buffer content. The results obtained from different techniques are consistent and show similar trends.
© 2007 Elsevier Ltd. All rights reserved.

Keywords: Hydroxypropylmethylcellulose; Simulated body fluids; Sol–gel transition; Differential scanning calorimetry

1. Introduction

Thermoreversible hydrogels have been extensively used in drug delivery systems (Hoffman, 2002; Jeong, Bae, Lee, & Kim, 1997). The most significant feature of thermoreversible hydrogels is that they undergo a reversible sol–gel transition over a certain temperature region (Gariepy & Leroux, 2004). Among these thermoreversible hydrogels, cellulose esters, especially methylcellulose (MC) and hydroxypropylmethylcellulose (HPMC) are most interesting due to the fact that they are naturally derived cellulose, which is one of the richest natural polymers on Earth (Sarkar, 1979). In particular, the most commonly used hydrophilic carrier for oral-administered controlled drug release systems is HPMC. This is because it displays good compression characteristics and swelling properties. Moreover, it offers a high level of drug loading compared to methylcellulose (MC) (Kiil & Dam-Johansen, 2003). When HPMC matrix comes in contact with water, the polymer begins to swell and forms a protective gel around the tablet content leading to a sustained release of drugs (Ford, 1999). In addition to drug delivery, thermoreversible hydrogels have been most recently used as engineering scaffolds for tissue growth (Chen et al., 2006).

The gelation behavior of MC and HPMC aqueous solutions has been extensively investigated and various mechanisms have been proposed (Haque & Morris, 1993; Haque, Richardson, & Morris, 1993; Hirren, Chevillard, Desbrieres, Axelo, & Rinaudo, 1998; Kato, Yokoyama, & Takahashi, 1978; Kobayashi, Huang, & Lodge, 1999; Li et al., 2002; Takahashi, Shimazaki, &

* Corresponding author. Tel.: +65 67905954; fax: +65 67911859.
 E-mail address: mscjoshi@ntu.edu.sg (S.C. Joshi).

Yamamoto, 2001). It is widely accepted that the dominant phenomenon for gelation is the intermolecular association of hydrophobic groups on the polymer chains, leading to cross-linking and gel formation. However, Suzuki, Taniguchi, and Enomoto (1972) and Tanaka and Ishida (1995) proposed that both hydrophobic interactions and hydrogen bonds are related to gel formation of MC aqueous solution. On the other hand, there still exists some controversy about the details of the hydrophobic association and the nature of junction zones formed in the gelation process (Kato et al., 1978; Takahashi et al., 2001). As suggested by many researchers, the thermogelation of MC and HPMC is dominantly caused by the hydrophobic interaction between the hydrophobic substitutions (Haque et al., 1993; Hirren et al., 1998; Li et al., 2002). All these explanations are not mutually supportive since these studies describe different aspect of gelation based on different experimental techniques. Moreover, although the key role of hydrophobic interaction in the thermogelation has been widely identified, the role of interchain hydrogen bonding in gelation is still controversial.

The behavior of hydrogels during thermogelation can be substantially altered by the addition of additives such as salts (Cho, An, & Song, 2006; Joshi & Lam, 2006; Kundu & Kundu, 2001; Nyström, Kjniksen, & Lindman, 1996; Sarkar, 1979). The salts can either reduce the water solubility of solutes (salting-out effect) or increase it (salting-in effect). The effects of cations are smaller than that of anions. A typical salting-out anions order is $SCN^- < ClO_4^- < I^- < NO_3^- < Br^- < Cl^- < F^- < HPO_4^- < SO_4^{2-}$. This phenomenon has been commonly known as Hofmeister series (Collins, 1997; Durme, Rahier, & Mele, 2005; Hofmeister, 1888). The Hofmeister series is of great interest as salts are commonly present in bio-systems, especially body fluids, which may affect the performance of hydrogels in applications like the oral controlled drug release systems. Fewer studies have been reported so far on the gelation behavior of HPMC in physiological environment such as simulated gastric fluid (SGF) and simulated intestinal fluid (SIF), which are always present in actual bio-applications.

The main objective of this study is to investigate the effects of physiological buffer on the thermogelation behavior of HPMC. Thermal properties of HPMC in SIF were firstly investigated. The solution isotopic effects on the thermal properties were measured with various mole ratios of Deuteraed water to deionized water ($D_2O:H_2O$) to study the hydrogen bonding. Thermodynamic data such as enthalpy, entropy and peak temperature obtained from thermal analysis provided important information on the interactions involved in the sol–gel transition. Rheological measurements were carried out to study the viscoelastic properties of HPMC solutions. The effects of polymer concentration and the gelation behavior of HPMC in aqueous solution were also studied and used as comparison.

2. Experimental

2.1. Materials

Hydroxypropylmethylcellulose (HPMC) was purchased from Sigma–Aldrich Inc., and was dried under vacuum at 60 °C and then stored in a desiccator before use. The specifications indicate that the number average molecular weight (M_n) is 10,000 g/mol, and the viscosity of a 2 wt% solution is 6 cps at 20 °C. The average degree of substitution (DS) of methyl and hydroxypropyl is 1.8–2.0 and 0.2–0.3, respectively. Deuteraed water (D_2O, 99.9%, Aldrich) was used without further purification. Sodium chloride (NaCl), monobasic potassium phosphate (KH_2PO_4), hydrochloride (HCl, 1 N) and sodium hydroxyl (NaOH, 1 N) were analytical grade and purchased from Sino Chemical Co., Ltd., SIF, without pancreatin, was prepared using KH_2PO_4 and NaOH. SGF, without pepsin, was prepared using NaCl and HCl according to the specification given in United States Pharmacopeia (The United States Pharmacopeia (25th ed.). US Pharmacopeial Convention Inc. & MD, 2002). The compositions of the various buffer solutions are listed in Table 1. For the SIF buffer solutions with different pH values (5.8, 6.6, 7.4, 7.8), they were prepared using 0.05 M KH_2PO_4; NaOH was added to adjust pH values. For the SIF buffer solutions with different pH values but with the same buffer content (8.6 g/L), NaCl was added to keep the buffer content constant. Unless mentioned otherwise, the pH of SIF used was 7.4 and the solvent was H_2O. The pH of SGF was 1.2, where the concentration of HCl was 70 mM and NaCl was added to tune the buffer content. The HPMC solutions were prepared by dissolving the polymer into respective buffer solutions and then stored in a refrigerator (4 °C) for 24 h before use.

Table 1
Compositions of SGF and SIF solutions

	SGF content (pH 1.2) (g/L)				SIF content (pH 7.4) (g/L)			
	4.6	9.2	18.4	32.2	8.3	16.6	24.9	33.2
NaCl (mM)	34.0	114.0	270.0	506.0				
HCl (mM)	70.0	70.0	70.0	70.0	–	–	–	–
KH_2PO_4 (mM)	–	–	–	–	50.0	100.0	150.0	200.0
NaOH (mM)	–	–	–	–	38.0	76.0	114.0	152.0

2.2. Micro-differential scanning calorimetry

Differential scanning calorimeter (micro-DSC MC-2 microcalorimeter, MicroCal Inc., USA) was used to study the thermodynamic properties of HPMC in various buffer solutions. Sample solution (0.5158 ml) and an equal amount of solvent as a reference were hermetically sealed into the sample cell and reference cell, respectively. Cooling and heating (at a rate of 1.0 °C/min) DSC curves were recorded in the temperature range of 20–90 °C. The values of thermodynamic parameters such as relative Cp, enthalpy changes (ΔH) and entropy changes (ΔS) were normalized for 1 L of sample volume by multiplying the original data by a factor of 1000 ml/0.5158 ml, where 0.5158 ml was the sample volume.

2.3. Molecular weight determination

The number average molecular weights (M_n) of the polymers were determined by a gel permeation chromatography (GPC) (Waters 2690, MA, USA) with a differential refractometer detector (Waters 410, MA, USA). The mobile phase used was DI water with a flow rate of 1 ml/min. Polymer sample (10 wt% in 4.6 g/L SGF buffer) was diluted 6 times and the solution was then filtered. Weight and number average molecular weights were calculated from a calibration curve using a series of Dextran standards (Aldrich, USA, with molecular weight ranging from 667 to 778,000).

2.4. Clouding point measurement

Light transmittance of HPMC solution (10 wt%) at various temperatures was measured at 500 nm using a UV–vis spectrometer (Jasco V-570, Japan). The heating rate was controlled at 1 °C/min by a Peltier-type temperature controller. The LCST values were determined at the temperatures showing an optical transmittance of 50%.

2.5. Rheological measurements

A stress controlled type rheometer (ARES 100FRTN1, Rheometric Scientific) was used to measure the flow properties and dynamic viscoelasticity of HPMC solutions. The rheometer is equipped with two sensitive force transducers for torque measurements ranging from 0.004 g cm to 100 g cm. The sample solution was poured between the parallel-plates (50 mm in diameter) and then a small amount of silicone oil was applied at the periphery of the solution to prevent evaporation. The dynamic storage modulus (G') and loss modulus (G''), were examined as a function of temperature from 20 °C to 75 °C with a strain amplitude (γ) of 5% (within the linear viscoelastic region), at a frequency (ω) of 1 rad/s and a heating rate of 1 °C/min. Isothermal frequency sweeps ($\omega = 0.1$–100 rad/s) on HPMC solutions were also performed at 5% strain.

3. Results and discussion

3.1. Thermal properties

3.1.1. Influence of SIF and SGF on the peak temperature (T_{max})

The thermograms of a 10 wt% aqueous solution of HPMC and that of HPMC containing SIF (8.3 g/L) in two solvents (H_2O and D_2O) are presented in Fig. 1. This concentration was used as a typical example because it could form strong gel as shown later. Thermograms with similar patterns were also observed for HPMC containing SGF but data are not shown in the paper to avoid repetition. In order to examine the degradation effect of SGF on the thermal gelation of HPMC, molecular weight of HPMC in SGF (4.6 g/L) before and after micro-DSC experiment were measured using GPC. The M_n of HPMC measured before and after the micro-DSC experiment was 8.1 K and 8.3 K, respectively, indicating that there was no degradation of HPMC in SGF during the experiments.

For comparison, the thermograms in H_2O were introduced first. The curve patterns for HPMC in SIF were found to be similar to those in aqueous solution. However, the T_{max}, defined as sol–gel transition temperature (Li et al., 2002), shifted to a lower temperature. For example, T_{max} for the endothermic curve was 66.0 °C in aqueous solution while it was 59.2 °C in the presence of SIF (8.3 g/L). During the heating process, a broad endothermic peak was observed while two exothermic peaks (a broad exothermic peak and a small shoulder) were present during the subsequent cooling process.

The similarities between the patterns of the thermograms for HPMC in the presence of SIF and in aqueous solutions indicate that they share the same mechanisms as described previously (Haque et al., 1993; Sarkar, 1979). It has been well known that the formation of intermolecular hydrogen bonding between hydroxyl groups of HPMC chains and water molecules as well as water cages
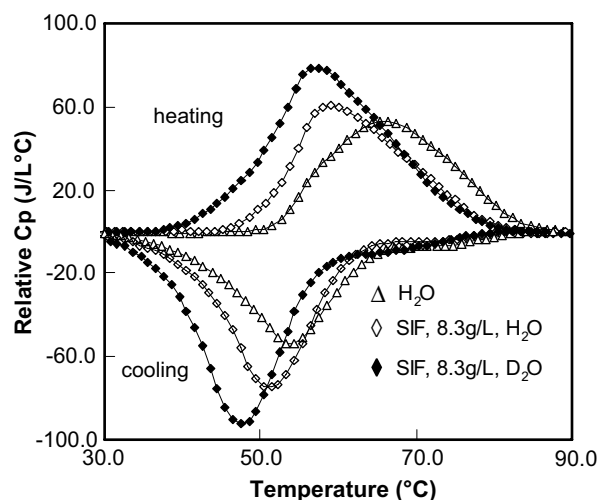

Fig. 1. Thermal properties of HPMC (10 wt%) in various solutions.

surrounding hydrophobic clusters of HPMC chains such as methoxyl substituted and relatively less hydrophobic hydroxypropyl substituted regions makes HPMC soluble at low temperature (Haque et al., 1993). The concept of water cages may be defined as the formation of enhanced water–water hydrogen bonding in the hydrophobic hydration shell (Maeda, Nakamura, & Ikeda, 2001). The intermolecular hydrogen bonding is gradually weakened with increasing temperatures. Upon heating to a temperature to the onset of the endothermic peak (T_{onset}), the water cages start to deform and break to expose the hydrophobic substitutions to the aqueous environment. The exposed hydrophobic substitutions form hydrophobic aggregation domains via hydrophobic–hydrophobic interactions. These domains are connected through hydrophobic groups yielding a three-dimensional physical network of HPMC chains.

It is worth noting that the endothermic peak (Fig. 1) and T_{max} (Table 2) shifted to a lower temperature, as compared with the aqueous solution of HPMC, in the presence of SIF (8.3 g/L) and SGF (4.6 g/L), indicating that the sol–gel transition was promoted and occurred early due to the added buffer. To interpret the buffer effect on the sol–gel transition in this study, it is important to consider the effect of salt on the water structure. As shown in Table 1, the compositions of SIF contain OH^- and $H_2PO_4^-$ while those of SGF contain Cl^-, which are water structure makers or salting-out anions according to the Hotmeister series. In their presence, the adjacent water molecules were polarized and rearranged in the electric field of the ion (Hribar, Southall, Vlachy, & Dill, 2002). Viscosity B coefficient is always used as an empirical constant representing ion–water interaction. Viscosity B coefficients of OH^- and $H_2PO_4^-$ are 0.112 L mol^{-1} and 0.34 L mol^{-1}, respectively (Marcus, 1997). Ions with positive viscosity B coefficient value are strong structure makers for water (Hribar et al., 2002). The structure makers have a tendency to attract water molecules around them, facilitating the sol–gel transition. This salting-out effect was induced via the following two ways (Freitag & Garret-Flaudy, 2002; Jeong, Bae, & Kim, 1999; Yuan, Wang, Han, & Wu, 2006; Zhang, Furyk, Bergbreiter, & Cremer, 2005). One is that the anions compete for water molecules and the water molecules are rearranged in the electric field of the anion. Less free water molecules are available to solvate polymers. The intermolecular hydrogen bonding was therefore weakened and easily disrupted. Another one is that the surface tension of the water cages surrounding the hydrophobic clusters

increased due to the salting-out effects of OH^- and $H_2PO_4^-$, causing depletion in the strength and number of water cages and resulting in enhanced hydrophobic association at low temperatures.

The broad exothermic peak and a smaller shoulder observed during the cooling process indicated that gel–sol transition proceeded in two successive transitions. Similar trends in thermograms of HPMC and MC in aqueous solutions have been reported by Hirren et al. (1998), yet their interpretations are different. The exact mechanisms cannot be obtained with thermograms alone, which will be elucidated via the viscoelastic study during the cooling process as shown later. In the presence of SIF, the gel–sol transition was deferred during the cooling process. This is due to the competition for the free water molecules by salting-out salts.

3.1.2. Influence of solvent

Although a fairy detailed picture of hydrophobic association involved in the thermogelation has been obtained, the effect of the interchain hydrogen bonding involved in the thermogelation of HPMC is not clear yet. Since Deuterium substitution is a very useful method to investigate the properties of hydrogen bonding interactions, this effect was studied using various molar ratios of D_2O and H_2O. As seen in Fig. 1, the patterns of thermograms of solutions of HPMC containing SIF in both solvents are very similar. However, the T_{max} in D_2O moved to a lower temperature. More interestingly, the T_{max} has a roughly linear relationship with the mole fraction of D_2O (Fig. 2a).

These observations are in contrast to the cases of poly(N-isopropylacrylamide) (PNIPAAm) studied by Kujawa and Winnik (2001), where the T_{max} value with D_2O is higher by 2 °C compared to that with H_2O. This increase of T_{max} for PNIPAAm can be explained as follows. It is well established that the deuterium bonding in D_2O is about 5% stronger than the hydrogen bonding in H_2O, leading to an increase in the T_{max} (Kujawa & Winnik, 2001; Zhang et al., 2005). Additionally, polymer chains are more extended in D_2O.

The opposite results obtained in our investigations for HPMC in the absence of SIF (data not shown) and in the presence of SIF indicated that interchain hydrogen bonding was involved in the gelation process, leading to a salting-out effect. In the case of HPMC, the decrease of T_{max} in D_2O was assumed to be due to the interchain hydrogen bonding rather than the combined effects of the

Table 2
Thermal properties of thermograms for HPMC SIF solutions with different pH values

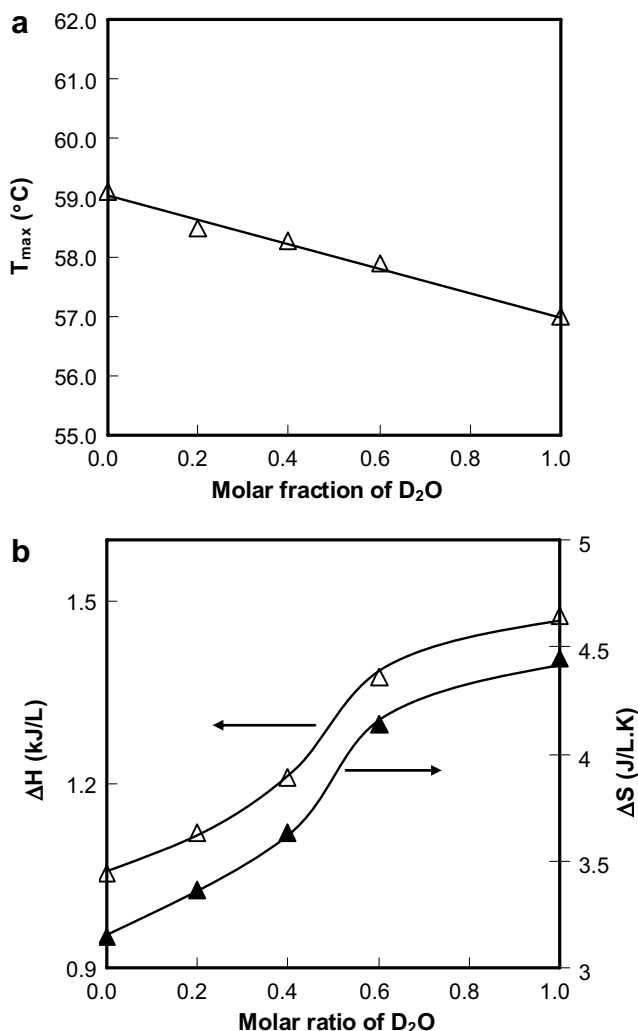|	SIF buffer with different pH				SIF buffer with constant buffer content (8.6 g/L)			
	pH 5.8 (6.9 g/L)	pH 6.6 (7.5 g/L)	pH 7.4 (8.3 g/L)	pH 7.8 (8.6 g/L)	pH 5.8	pH 6.6	pH 7.4	pH 7.8
T_{max} on heating (°C)	61.69	60.90	59.17	58.98	60.73	60.54	59.05	58.98
T_{max} on cooling (°C)	51.24	51.15	49.87	49.78	50.54	50.35	49.75	49.78
ΔH on heating (kJ/L)	0.94	0.95	0.996	1.03	0.95	0.96	1.00	1.03
ΔS on heating (J/L K)	2.79	2.86	2.97	3.08	2.82	2.87	2.98	3.08

Fig. 2. Thermodynamic properties of HPMC solutions (10 wt%, SIF 8.3 g/L) as a function of molar fractions of D_2O. (a) T_{max}; (b) enthalpy and entropy changes (ΔH and ΔS).

interchain hydrogen bonding and enhanced hydrophobic interactions. This is because a non-linear change in the T_{max} with D_2O content instead of a linear change will be observed if D_2O has more than two types of complex interactions with HPMC (Mao et al., 2004). This trend is consistent with the findings reported by Winnik (1989) for hydroxypropyl cellulose (HPC).

In addition to T_{max}, enthalpy and entropy changes (ΔH and ΔS) with various D_2O content were extracted from thermograms and the results are illustrated in Fig. 2b, where ΔH was calculated by integrating the area under the curves between the T_{onset} and T_{offset} (the end temperatures for the endothermic peak) while ΔS was calculated using equation

$$\Delta S = \int_{T_{onset}}^{T_{offset}} (C_P/T) \mathrm{d}T.$$

It was interesting to find that these thermodynamic parameters exhibited a significant dependence on D_2O content

and followed sigmoidal shape with the variations in D_2O content. Three distinct regions were observed. When the molar ratio is below 0.4, ΔH and ΔS increased slightly. They underwent a rapid increase in the region where $0.4 <$ molar ratio < 0.6, and then gradually reached a plateau. To interpret this trend, it is necessary to investigate the thermodynamic parameters of HPMC containing SIF in H_2O. There are several processes that might consume or release heat during thermogelation. For instance, heat was consumed to break intermolecular hydrogen bonding and water cages as well as for hydrophobic association. However, the formation of interchain hydrogen bonding is an exothermic process. It has been extensively studied and demonstrated that the positive ΔH (endothermic peak) was mainly related to destruction of water cages around hydrophobic clusters of the polymer chains (Alexandridis & Holzwarth, 1997; Feil, Bae, Jan, & Kim, 1993; Otake, Inomata, Konno, & Saito, 1990). Therefore, ΔS must be positive at a given temperature to meet the requirement of $\Delta G = \Delta H - T\Delta S < 0$, where $\Delta H > 0$. The ΔS caused by the formation of gel network is negative resulting from the reduction in the flexibility of polymer chains. In addition, water molecules get trapped into these gel networks, leading to a negative ΔS. Such inconsistence can be resolved by consideration for smaller molecules such as water molecules; these are smaller in size but large in numbers. The water molecules involved in hydrogen bonding and water cages are relatively ordered at low temperature and become disordered upon destruction at high temperatures. More importantly, this positive ΔS value is greater than that of the negative ones to make the total ΔS value positive, as demonstrated in Fig. 2b. This phenomenon is in line with those reported by many other researchers (Alexandridis et al., 1997; Haque et al., 1993). The addition of SIF (8.3 g/L) also induces a slight increase in ΔH and ΔS compared to those in the absence of SIF as shown later.

In D_2O, it was expected that more heat be consumed to break the strengthened intermolecular hydrogen bonding. On the other hand, this is compensated by the formation of interchain hydrogen bonding because the later is prevalent in D_2O. The increase of ΔH and ΔS in D_2O compared to those in H_2O can only be explained by consideration of the small molecules including water molecules and ions surrounding hydroxyl groups of the HPMC chains (Fig. 3a). Similar results have been reported by Weng, Zhang, Ruan, Shi, and Xu (2004) where small molecules acted as an overcoat surrounding a cellulose chain. In our cases, the small molecules served as a shell to the hydroxyl groups at low temperatures, preventing the formation of interchain hydrogen bonding. This is very similar to the water cages surrounding hydrophobic clusters as stated earlier. The shells disturbed and broke to expose hydroxyl groups at raised temperatures, leading to the formation of interchain hydrogen bonding (Fig. 3b). It may be therefore suggested that the both interchain hydrogen bonding and hydrophobic interactions are concerned with the gelation of HPMC, while the later plays a more important role in the gelation.
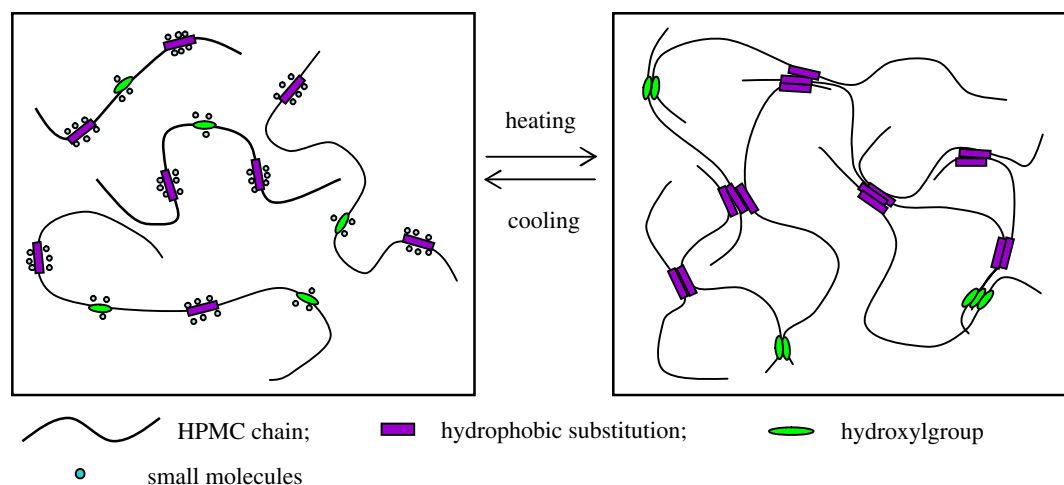
Fig. 3. Schematic structures of the sol–gel transition of HPMC aqueous solutions with buffer.

The junction zones also contain two parts: association of hydroxyl groups and hydrophobic clusters as illustrated in Fig. 3b. This conclusion is in agreement with the studies performed on MC (Suzuki et al., 1972).

Now, the three regions trend of ΔH with various D_2O content (Fig. 2b) can be explained in terms of the strength of the shell for the hydroxyl groups. The first region indicated that the strength of the shell increased slowly, where more heat was consumed to break the shell to induce association of hydroxyl groups of HPMC chains. The second region suggested that the strength of the shell increased rapidly, where much more heat was needed. When the molar ratio of D_2O was higher than 0.6, the absorbed heat gradually reached a plateau. This indicated that the rate of increase in the shell strength decreased gradually approaching zero. It is interesting to note that the same trend was seen for the ΔS. This further confirmed that the changes in enthalpy and entropy were related to the strength of the shell.

3.1.3. Influence of buffer content

With the increase in either SGF or SIF content, the DSC curves became broader (data not shown) and the T_{max} shifted nearly in a linear manner to lower values with the two curves fitted with their slopes as $-0.42\,°C\,g^{-1}\,L$ and $-0.63\,°C\,g^{-1}\,L$, respectively; refer Fig. 4a. The more pronounced salting-out effect with increasing buffer content is because of the fact that buffers with higher concentrations can attract more free water molecules around the salt ions, resulting in fewer free water molecules available around the hydrophobic clusters and hydroxyl groups. The water cages around the hydrophobic clusters and the shell around the hydroxyl groups were further weakened with the increasing buffer content upon heating. Similarly, the re-formation of cage structure around the methyl groups was further deferred with high buffer content during the cooling process (data not shown).
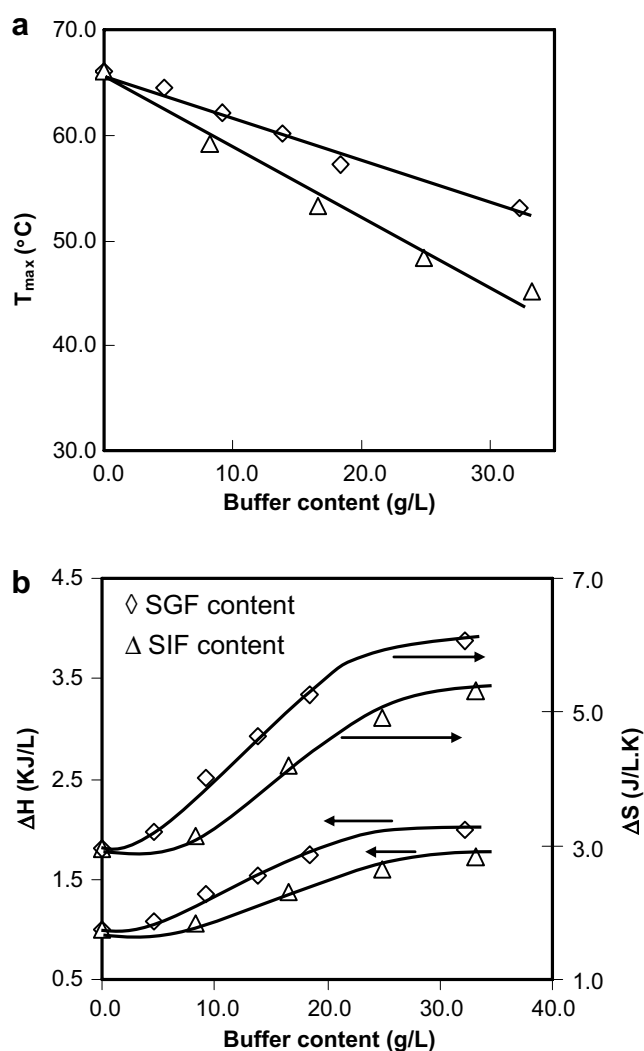

Fig. 4. Thermodynamic properties of HPMC solutions (10 wt%, SIF 8.3 g/L) as a function of buffer content. (a) T_{max}; (b) enthalpy and entropy changes (ΔH and ΔS).

The T_{max} curve for the SIF has a higher negative slope indicating that it has a stronger salting-out effect compared

to that of SGF. This result can be explained by the difference in the salting out capacity of the anions since cations have much less effect on the thermogelation compared to anions. The value of the viscosity B coefficient of Cl^- is -0.005 L mol^{-1}, which is less than those of OH^- and $H_2PO_4^-$ (Marcus, 1997). Anions with higher viscosity B coefficient values tend to attract water molecules from polymers, water cages and shells more strongly. Therefore, salting-out effect is more pronounced in the presence of SIF.

The effects of buffer content on ΔH and ΔS are illustrated in Fig. 4b. It was observed that all curves are of sigmoidal shape. The plots can be divided into three buffer content regions. For SIF, below 8.3 g/L, and above 24.9 g/L, ΔH and ΔS exhibit a slight increase with the increasing SIF content. However, these quantities undergo a sharp increase in the regions ranging from 8.3 g/L to 24.9 g/L. Similar trend has also been reported by Alexandridis et al. (1997) for pluronics showing that ΔH reached a plateau at higher salt concentrations. We also showed that some heat was consumed to break the shell around the hydroxyl groups of the polymer chains. However, endothermic heat was mainly attributed to the destruction of water cages around hydrophobic clusters of the polymer chains (Alexandridis et al., 1997; Durme et al., 2005; Li et al., 2002). In addition, the strength of the water cages reduced with the increasing buffer content. Therefore, such trends can only be explained in terms of the total number of hydrogen bonding in the water cages. This can be explained as follows. Firstly, because the distribution of methoxyl and hydroxypropyl along HPMC chains is not homogenous, it may contain trisubstituted, disubstituted and monosubstituted units. The thermogelation of HPMC was mainly attributed to the hydrophobic interactions of trimethoxyl substitutions (Hirren et al., 1998). Secondly, lower-methoxyl substituted units and less hydrophobic substitutions such as hydroxypropyl groups become more hydrophobic in the presence of SGF and SIF due to the salting-out effects. Hence, the total number of higher hydrophobic substitutes increased. On the other hand, more new water cages are formed around these less substituted units at lower temperatures. Therefore, more energy will be needed to break these new water cages to induce hydrophobic association in addition to the highly substituted units. The sigmoid trend in Fig. 4b can be interpreted in the following ways. The number of newly formed water cages increased slightly at low buffer content. It is possible to assume that salts at low concentrations mainly compete for free water molecules in bulk water instead of those in polymer–water interface. However, as the buffer content continued to increase and reached 24.9 g/L, there are enough anions to compete for a lot of water molecules in the polymer–water interface and create more hydrophobic substitutions, resulting in a rapid increase in the number of newly formed water cages. Furthermore, the number of newly formed water cages gradually reached saturation when the SIF content was above 24.9 g/L, resulting in a

slight increase in ΔH. The similar observation for ΔS further confirmed that ΔH was mainly related with the number of newly formed water cages. This is because ΔS was also mainly attributed to the disruption of water cages as elaborated earlier in this study. It is also noted that the ΔH and ΔS values in the case of SGF were a little higher than those for SIF.

3.1.4. Influence of pH

The effect of pH on the thermogelation is of interest since orally administrated drug loaded hydrogels are exposed to SGF (pH between 1.0 and 2.5) and followed by SIF (pH between 5.5 and 7.9) (Masaru, Masaharu, Takeshi, & Ryoichi, 1999). As shown in Table 2, upon heating the T_{max} decreased slightly with increasing pH. This was caused by the slight increase in the NaOH concentration because NaOH adjusted the pH. In the case of SIF with equal salt content, the similar trend was also observed. This was because the salting-out ability of OH^- is more pronounced than that of Cl^-. The corresponding ΔH and ΔS of HPMC in buffers with different pH values are illustrated in Table 2. They all increased slightly with increasing pH, indicating that they exhibited weak pH dependence. Unlike polyelectrolytes, non-ionic polymers such as HPMC will not ionize by changing the pH. Hence, the thermal properties were not affected greatly by the pH. This finding is in agreement with some reported studies (Mitchell et al., 1990).

3.1.5. Influence of polymer concentration

In addition to the parameters mentioned earlier, the effect of polymer concentration on thermal behavior was examined (data not shown). The influence of polymer concentration ranging from 1 wt% to 10 wt% on the T_{max} was not significant, indicating the gelation process was a temperature driven process rather than only driven by the heat input (Lam, Joshi, & Tan, 2007). On the other hand, ΔH and ΔS were found to be linearly proportional to the polymer weight concentration, suggesting that more HPMC chains were involved in the gelation. Similar results are also found for HPMC in the absence of buffer.

3.2. Changes in light transmittance

Transmittance changes for HPMC aqueous and buffer solutions as a function of temperature are presented in Fig. 5. The solutions were transparent below the T_{onset} but became turbid at temperatures (LCST) between the T_{onset} and T_{max} measured by the micro-DSC. During cooling, the solution became transparent at low temperatures. However, an obvious hysteresis was observed during the cooling process. The results are consistent with those obtained using the micro-DSC. It should be mentioned that the LCST was relatively independent of concentration in the studied range. However, the LCST of diluted HPMC solution (3 wt% and less) was found to increase by a few degrees. For instance, the LCST of HPMC solution
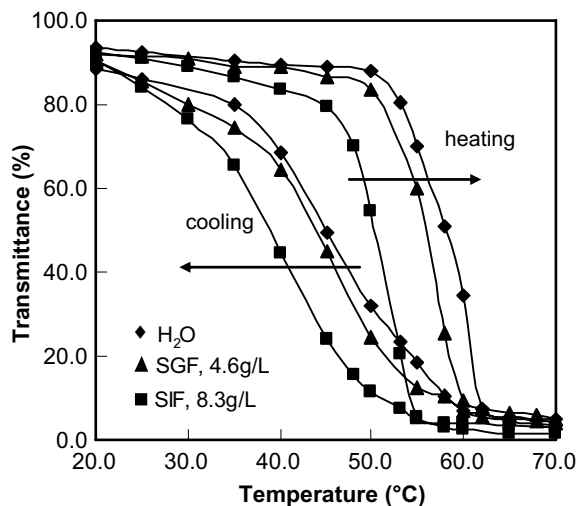
Fig. 5. Light transmittance of HPMC solutions (10 wt%) in various solutions as a function of temperature.

Fig. 6. Concentration dependence of G_E for HPMC in the presence of SIF (8.3 g/L) (frequency $\omega = 0.1$ rad/s, strain amplitude $\gamma = 5\%$ and 68 °C).

(1 wt% in DI water) was 69.0 °C. The reason for this is that the polymer aggregates are slow to aggregate to a size that can be detected by the UV–vis at low concentrations. The gelation behavior induced by temperature is known as the sol–gel transition with a LCST. The LCST moved to a lower temperature in the presence of SGF and SIF. The turbidity was attributed to the Rayleigh scattering from junctions formed in the gelation process. LCST is always considered as an indication of phase separation (Schild, 1992).

The relationship between gelation and phase separation for MC and HPMC has been elaborated by other researchers in their studies (Kobayashi et al., 1999; Sarkar, 1979; Takahashi et al., 2001). However, there are different opinions about the nature of the phase separation and gelation. For instance, Kobayashi et al. (1999) showed that the gelation was accompanied by liquid–liquid phase separation, as evidenced by the turbidity changes. Takahashi et al. (2001) suggested a concurrence of phase separation and gelation. He also pointed out the possibility of gel–gel phase separation with different polymer concentrations at higher temperatures. Many other researchers proposed that the turbidity was caused by the hydrophobic interactions of the methoxyl groups on the polymer chains (Sarkar & Walker, 1995). In our investigation, no precipitation was observed up to 75 °C. More importantly, the decrease in gel elastic strength (G') at the LCST accompanied by the phase separation was not observed as seen in Fig. 6. It is therefore suggested that the turbidity is more likely be due to micro-phase separation induced by hydrophobic association and hydroxyl group association. The micro-phase separation would in turn cause gelation rather than macro-phase separation because there is no precipitation. This phenomenon is in agreement with an observation made by Li et al. (2002) in their studies about the formation of MC gel or microgel when the temperature was above the LCST.
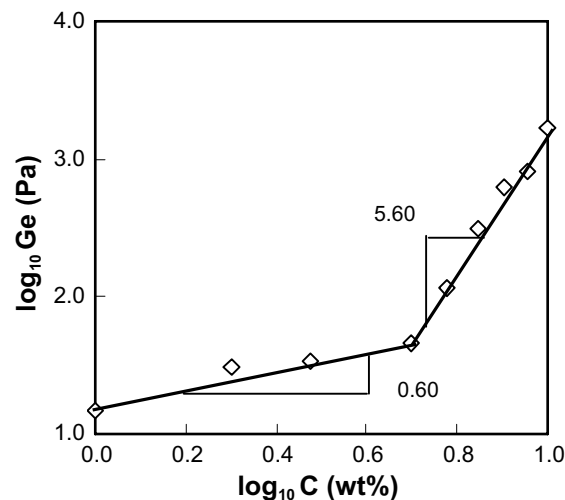
3.3. Viscoelastic studies

The viscoelastic properties of HPMC solutions were investigated to further understand the gelation mechanism. SIF was chosen as a typical example since HPMC in SGF and in SIF exhibited similar behavior. Additionally, changing pH did not generate significant difference on the properties of HPMC, as evidenced earlier. The concentration dependence of the quasi-equilibrium modulus G_E was examined at a gelling temperature of 68 °C for HPMC solutions in the presence of SIF, where G_E was defined as the storage modulus (G') at the frequency of 0.1 rad/s. A scaling relation $G_E = \varepsilon^s$ has been widely used to characterize the gel state, where ε is the relative distance of a variable such as concentration or temperature from the sol–gel transition point, and s is the exponent (De Gennes, 1997). In this study, ε was defined as concentration instead of relative distance of concentration because the critical concentration for sol–gel transition at this temperature is difficult to obtain as pointed out by Li (2002) in his work. As seen in Fig. 6, the slopes of the two straight-line segments were 0.6 and 5.6, respectively. The results suggested that the gels formed at concentrations below 5 wt% were weak gels while those formed above 5 wt% were strong gels. It should be noted that the definition of weak (<5 wt%) and strong gel (>5 wt%) was based on the scaling relations found from equation of $G_E = \varepsilon^s$. Similar results can be found in studies elsewhere, suggesting that the multi-scaling laws for the gelation of MC were due to its heterogeneous gelation network (Lee, Cho, & Park, 2005; Li, 2002).

The temperature dependence of G' for HPMC (10 wt%) in the presence of SIF (8.3 g/L) was also studied (Fig. 7). It was found that the gelation proceeded in two stages. G' increased slightly with increasing temperature up to about 51 °C. This may be attributed to the entanglements of HPMC chains. On further heating, G' increased sharply before attaining a near plateau after
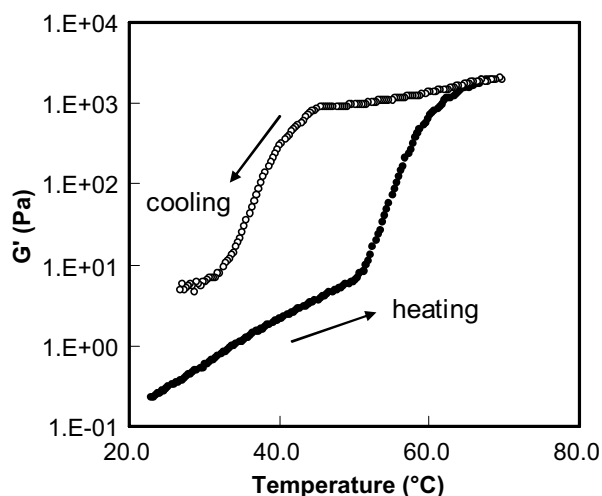
Fig. 7. Dynamic storage modulus G' of HPMC (10 wt%) in the presence of SIF (8.3 g/L) at a frequency $\omega = 1$ rad/s and a strain amplitude $\gamma = 5\%$.

Fig. 8. G_E of HPMC solutions as a function of SIF content (frequency $\omega = 0.1$ rad/s, strain amplitude $\gamma = 5\%$ and 68 °C).

about 62 °C. It was observed that the rapid increase of G' was related to the temperature region between T_{onset} and T_{max} measured by micro-DSC. The reason for such a rapid increase in G' at temperatures greater than the T_{onset} is kinetics of the sol–gel transition, where heat was first absorbed to break the water cages and the shell surrounding the hydrophobic clusters and hydroxyl groups, respectively. This was followed by hydrophobic association and hydroxyl groups association as illustrated in Fig. 3. The rapid increase in G' for HPMC gel was caused by the development of network of junction zones of hydrophobic association and hydroxyl groups association. Finally, G' reached a plateau when the formation of the gel network was mostly completed. During subsequent cooling, G' decreased slowly in contrast to the rapid increase of G' in the same temperature zone upon heating. The initial slow reduction in G' was due to the gradual weakening of the network, described by the smaller shoulder at higher temperatures. The subsequent rapid decrease in G' corresponded to the large amount of heat released by the formation of the water cages, shells and intermolecular hydrogen bonding during the dissociation of the gel network. The pattern of G' upon heating is very similar to that in the absence of buffer (data not shown). However, G' decreased gradually during the whole cooling process in the absence of buffer. The reason for the gel in aqueous solution for not able to retain its strength is because the gel network is easily weakened in the presence of hydroxypropyl groups even at higher temperatures. In the presence of SIF, the dissociation of gel structure, re-formation of intermolecular hydrogen bonding, water cages and shells were deferred in the cooling process. This is due to the competition for the free water molecules by salting-out salts. G' curve further moves to a lower temperature upon heating with the increasing SIF contents (data not shown). The salting-out effect is consistent with those measured by micro-DSC.
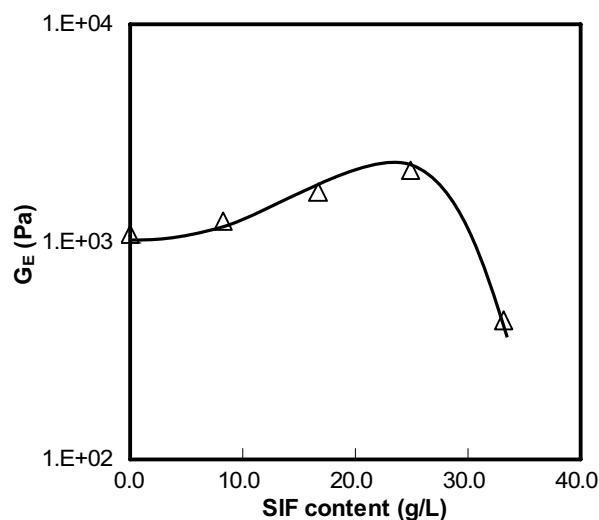
To compare the viscoelastic properties of the polymers in different SIF content solutions, frequency dependence for HPMC (10 wt%) was conducted at 65 °C. G' was much greater than G'' (loss modulus) and showed a weak dependence over the whole frequency range. This behavior is typical for a gel. G_E values are illustrated in Fig. 8. It was found that the gel elasticity (G_E) increased slightly with the initial increase in SIF content. This is because the presence of salting-out salts led to a stronger hydrophobic association and hydroxyl group association. This result is in good agreement with that reported by Sarkar (1979). It should be noted that G_E increased rapidly when SIF content increased from 8.3 g/L to 24.9 g/L. This trend is similar to those for the ΔH and ΔS as stated earlier and can be explained by the cross-linking density of the physical network. The total number of higher hydrophobic substitutes increased with increasing SIF content in a sigmoidal manner, resulting in a similar trend in the changes of the cross-linking density. However, G_E decreased significantly when SIF content further increased to 33.2 g/L. This was caused by the macroscopic phase separation induced by this high salinity.

4. Conclusions

Thermogelation of HPMC solutions in the presence of SGF/SIF with different content has been systematically investigated with micro-DSC, UV–vis and rheological techniques. Micro-DSC studies revealed that both SGF and SIF do not change the mechanisms of sol–gel transition of HPMC, but their presence promoted the sol–gel transition due to their salting-out effect without changing the gelation mechanism. These effects of combined salts (in SIF/SGF) follow Hofmeister series of salt ions. Their salting-out ability was due to the strengths of the interactions between the anions and water. The isotopic study

proved that the formation of interchain hydrogen bonding between hydroxyl side groups occurs during the gelation in addition to the hydrophobic interactions. It was noted that the effect of pH on the thermal properties was not significant. The sol–gel transitions of HPMC solutions are entropy driven processes. Moreover, the changes in endothermic enthalpy and entropy as a function of buffer content showed a sigmoidal trend with the increasing buffer content, which was mainly due to the change of the number of water cages. Turbidity was caused by the microscopic-phase separation, which, in turn, contributed to gelation. Rheological measurements showed that G_E at the gel state had different scaling relations to the polymer concentration. Moreover, G_E was affected by buffer content. Thus, it is possible to tailor the gel elasticity by varying the buffer content in addition to the polymer concentration. The temperature dependence of the viscoelastic behavior was in well agreement with the observed thermal behavior.

Acknowledgement

References

Alexandridis, P., & Holzwarth, J. F. (1997). Differential scanning calorimetry investigation of the effect of salts on aqueous solution properties of an amphiphilic block copolymer (Poloxamer). *Langmuir, 13*, 6074–6082.

Chen, C. H., Tsai, C. C., Chen, W. H., Mi, F. L., Liang, H. F., Chen, S. C., et al. (2006). Novel living cell sheet harvest system composed of thermoreversible methylcellulose hydrogels. *Biomacromolecules, 7*, 736–743.

Cho, Y. W., An, S. W., & Song, S. C. (2006). Effect of inorganic and organic salts on the thermogelling behavior of poly(organophosphazenes). *Macromolecular Chemistry and Physics, 207*, 412–418.

Collins, K. D. (1997). Charge density-dependent strength of hydration and biological structure. *Biophysical Journal, 72*, 65–76.

De Gennes, P. G. (1997). *Scaling concepts in polymer physics*. New York: Cornel University Press, Ithaca.

Durme, K. V., Rahier, H., & Mele, B. V. (2005). Influence of additives on the thermoresponsive behavior of polymers in aqueous solution. *Macromolecules, 38*, 10155–10163.

Feil, H., Bae, Y. H., Jan, F. J., & Kim, S. W. (1993). Effect of comonomer hydrophilicity and ionization on the lower critical solution temperature of N-isopropylacrylamide copolymers. *Macromolecules, 26*, 2496–2500.

Ford, J. L. (1999). Thermal analysis of hydroxypropylmethylcellulose and methylcellulose: Powders, gels and matrix tablets. *International Journal of Pharmaceutics, 176*, 209–228.

Freitag, R., & Garret-Flaudy, F. (2002). Salt effects on the thermoprecipitation of poly-(N-isopropylacrylamide) oligomers from aqueous solution. *Langmuir, 18*, 3434–3440.

Gariepy, E. R., & Leroux, J. C. (2004). In situ-forming hydrogels – review of temperature-sensitive systems. *European Journal of Pharmaceutics and Biopharmaceutics, 58*, 409–426.

Haque, A., & Morris, E. R. (1993). Thermogelation of methylcellulose. 1. Molecular-structures and processes. *Carbohydrate Polymers, 22*, 161–173.

Haque, A., Richardson, R. K., & Morris, E. R. (1993). Thermogelation of methylcellulose. 2. Effect of hydroxypropyl substitutents. *Carbohydrate Polymers, 22*, 175–186.

Hirren, M., Chevillard, C., Desbrieres, J., Axelo, M., & Rinaudo, M. (1998). Thermogelation of methylcellulose: New evidence for understanding the gelation mechanism. *Polymer, 39*, 6251–6259.

Hoffman, A. S. (2002). Hydrogels for biomedical applications. *Advanced Drug Delivery Review, 54*, 3–12.

Hofmeister, F. (1888). Zur lehre der wirkung der salze. Zweite mittheilung. *Archiv fuer Experimentelle Pathologie und Pharmakologie, 24*, 247–260.

Hribar, B., Southall, N. T., Vlachy, V., & Dill, K. A. (2002). How ions affect the structure of water. *Journal of the American Chemical Society, 124*, 12302–12311.

Jeong, B., Bae, Y. H., & Kim, S. W. (1999). Thermoreversible gelation of PEG-PLGA-PEG triblock copolymer aqueous solutions. *Macromolecules, 32*, 7064–7069.

Jeong, B., Bae, Y. H., Lee, D. S., & Kim, S. W. (1997). Biodegradable block copolymers as injectable drug-delivery systems. *Nature, 388*, 860–862.

Joshi, S. C., & Lam, Y. C. (2006). Modeling cellulose heat and degree of gelation for methyl hydrogels with NaCl additives. *Journal of Applied Polymer Science, 101*, 1620–1629.

Kato, T., Yokoyama, M., & Takahashi, A. (1978). Melting temperature of thermally reversible gels. IV Methyl cellulose-water gels. *Colloid Polymer Science, 256*, 15–21.

Kiil, S., & Dam-Johansen, K. (2003). Controlled drug delivery from swellable hydroxypropylmethylcellulose matrices: Model-based analysis of observed radial front movements. *Journal of Controlled Release, 90*, 1–21.

Kobayashi, K., Huang, C., & Lodge, T. P. (1999). Thermoreversible gelation of aqueous methylcellulose solutions. *Macromolecules, 32*, 7070–7077.

Kujawa, P., & Winnik, F. M. (2001). Volumetric studies of aqueous polymer solutions using pressure perturbation calorimetry: A new look at the temperature-induced phase transition of poly(N-isopropylacrylamide) in water and D$_2$O. *Macromolecules, 3*, 4130–4135.

Kundu, P. P., & Kundu, M. (2001). Effect of salts and surfactant and their doses on the gelation of extremely dilute solutions of methyl cellulose. *Polymer, 42*, 2015–2020.

Lam, Y. C., Joshi, S. C., & Tan, B. K. (2007). Thermodynamic characteristics of gelation for methyl-cellulose hydrogels. *Journal of Thermal Analysis and Calorimetry, 87*, 475–482.

Lee, S. C., Cho, Y. W., & Park, K. (2005). Control of thermogelation properties of hydrophobically-modified methylcellulose. *Journal of Bioactive and Compatible Polymers, 20*, 5–13.

Li, L. (2002). Thermal gelation of methylcellulose in water: Scaling and thermoreversibility. *Macromolecules, 35*, 5990–5998.

Li, L., Shan, H., Yue, C. Y., Lam, Y. C., Tam, K. C., & Hu, X. (2002). Thermally induced association and dissociation of methylcellulose in aqueous solutions. *Langmuir, 18*, 7291–7298.

Maeda, Y., Nakamura, T., & Ikeda, I. (2001). Changes in the hydration states of poly(N-alkylacrylamide)s during their phase transitions in water observed by FTIR spectroscopy. *Macromolecules, 34*, 1391–1399.

Mao, H. B., Li, C. M., Zhang, Y. J., Furyk, S., Cremer, P. S., & Bergbreiter, D. V. (2004). High-throughput studies of the effects of polymer structure and solution components on the phase separation of thermoresponsive polymers. *Macromolecules, 37*, 1031–1036.

Marcus, Y. (1997). *Ion properties*. New York: Marcel Dekker, Inc..

Masaru, Y., Masaharu, A., Takeshi, S., & Ryoichi, K. (1999). Thermo- and pH-responsive gels for application in colon delivery systems. *Radiation Physics and Chemistry, 55*, 677–680.

Mitchell, K., Ford, J. L., Armstrong, D. J., Elliott, N. C., Rostron, C., & Hogan, J. E. (1990). The influence of additives on the cloud point, disintegration and dissolution and hydroxylpropylmethylcellulose gels and matrix tablets. *International Journal of Pharmaceutics, 66*, 233–242.

Nyström, B., Kjniksen, A. L., & Lindman, B. (1996). Effects of temperature, surfactant, and salt on the rheological behavior in

semidilute aqueous systems of a nonionic cellulose ether. *Langmuir, 12*, 3233–3240.

Otake, K., Inomata, H., Konno, M., & Saito, S. (1990). Thermal-analysis of the volume phase-transition with *N*-isopropylacrylamide gels. *Macromolecules, 23*, 283–289.

Sarkar, N. (1979). Thermal gelation properties of methyl and hydroxy-propyl methylcellose. *Journal of Applied Polymer Science, 24*, 1073–1087.

Sarkar, N., & Walker, L. C. (1995). Hydration dehydration properties of methylcellulose and hydroxypropylmethylcellulose. *Carbohydrate Polymers, 27*, 177–185.

Schild, H. G. (1992). Poly(*N*-isopropylacrylamide)-experiment, theory and application. *Progress in Polymer Science, 17*, 163–249.

Suzuki, K., Taniguchi, Y., & Enomoto, T. (1972). The effect of pressure on the sol–gel transformations of macromolecules. *Bulletin of the Chemical Society of Japan, 45*, 336–338.

Takahashi, M., Shimazaki, M., & Yamamoto, J. (2001). Thermoreversible gelation and phase separation in aqueous methyl cellulose solutions. *Journal of Polymer Science: Part B: Polymer Physics, 39*, 91–100.

Tanaka, F., & Ishida, M. (1995). Thermoreversible gelation of hydrated polymers. *Journal of the Chemical Society, Faraday Transactions, 91*, 2663–2670.

The United States Pharmacopeia (25th ed.). US Pharmacopeial Convention Inc., Rockville, MD, 2002.

Weng, L. H., Zhang, L. N., Ruan, D., Shi, L. H., & Xu, J. (2004). Thermal gelation of cellulose in a NaOH/thiourea aqueous solution. *Langmuir, 20*, 2086–2093.

Winnik, F. M. (1989). Association of hydrophobic polymers in H_2O and D_2O-fluorescence studies with (hydroxypropyl) cellulose. *Journal of Physical Chemistry, 93*, 7452–7457.

Yuan, G. C., Wang, X. H., Han, C. C., & Wu, C. (2006). Reexamination of slow dynamics in semidilute solutions: Temperature and salt effects on semidilute poly(*N*-isopropylacrylamide) aqueous solutions. *Macromolecules, 39*, 6207–6209.

Zhang, Y. J., Furyk, S., Bergbreiter, D. E., & Cremer, P. S. (2005). Specific ion effects on the water solubility of macromolecules: PNIPAM and the Hofmeister series. *Journal of the American Society, 127*, 14505–14510.